

Supplementary Appendix

This appendix has been provided by the authors to give readers additional information about their work.

Supplement to: Radu A, Pichon C, Camparo P, et al. Expression of follicle-stimulating hormone receptor in tumor blood vessels. *N Engl J Med* 2010;363:1621-30.

Supplementary material

Methods

Tissue specimens.

Cancer tissues obtained from the “Val de Grace” Hospital, Paris, the “Henri Mondor” Hospital, Créteil, the “Tenon” Hospital, Paris, the “Beaujon” Hospital, Clichy, and the “Institut Mutualiste Montsouris”, Paris, were collected immediately after surgery. Paraffin sections were obtained from the Biorepository of the Mount Sinai School of Medicine, New York. The specimens were fixed in 10% formalin for 48 hours, cut in 5 mm thick tissue sections, washed thoroughly with PBS, dehydrated in graded ethanol and xylene, and embedded in paraffin. Large sections of 1.5-2.5 cm² were cut from the paraffin blocks. Several unfixed samples were frozen on dry ice and stored in liquid nitrogen until sectioning with a cryostat for immunofluorescence microscopy and/or immunoprecipitation and immunoblotting experiments.

Tissue microarrays (TMA)

The original slides were reviewed by the study pathologists (PC, MA, YA, AC, GF) and slides containing tumor or normally appearing tissue were selected and marked with coloured ink. TMA for prostate, breast, kidney, pancreas, and urinary bladder tumors were constructed using archived formalin-fixed paraffin embedded tissue.¹ For each patient, 3-4 cylindrical cores (0.6 mm in diameter) of tumor and 3-4 cores of normal (non-malignant, non dysplastic) tissue were transferred from the selected areas of the paraffin blocks to the recipient blocks. Each recipient block regrouped tumors for 28 to 48 patients. Large serial 5 µm-thick sections of the TMA blocks, containing all the cores, were cut and stained with haematoxylin-eosin. Images covering the full area of each core were obtained from one section of each TMA.

Immunohistochemistry

The sections were attached to SuperFrost slides, deparaffinized with toluene, gradually dehydrated in ethanol, and washed with running tap water for 60 min. Access to tissue antigen sites for antibody attachment was enhanced by incubating slides at 90°C for 40 min with 10 mM citrate buffer, pH 6. After cooling for 20 min at room temperature (RT) and after each subsequent step, slides were rinsed with PBS. To block endogenous peroxidase activity the sections were incubated with 6% hydrogen peroxide (15 min at RT). Sodium borohydride (10 mg/ml) was used to quench the free aldehyde groups (15 min). Non specific binding of antibodies was blocked by incubating slides with 2% goat serum in PBS (blocking buffer) for 2 hours at RT. The slides were incubated with 5 µg/ml FSHR323, or FSHR190, or FSHR225² in blocking buffer overnight at 4°C. Goat anti-mouse IgG (Fc-specific) coupled to horseradish peroxidase (Sigma, 1:200 dilution) was used as secondary antibody. As chromogen we used 3-amino-9-ethyl-carbazole (AEC; Sigma). The chromogenic development was monitored for 15 minutes through a light microscope. The sections were washed in distilled water and counterstained with Harris haematoxylin for 10 sec. The slides were mounted in Dako Glycergel mounting medium. For some patients none of the TMA cores contained vessels and for other patients the cores contained no stained vessels. As both these situations could have been caused by the insufficient sampling inherent to the small area of the TMA cores, large sections from the same patient have been analyzed. For 125 of the 773 patients prostate cancer patients we analyzed large sections. For the remaining patients we used TMA, which allowed simultaneous processing and direct comparison of sections from 28-48 patients on each microscope slide.

Indirect immunofluorescence confocal microscopy

Serial 7 μm cryostat sections of Tissue-Tek-embedded unfixed frozen prostates were collected on SuperFrost slides and air dried. The sections were fixed with 3% paraformaldehyde in PBS for 15 min at RT. The free aldehyde groups were quenched with 100 mM NH_4Cl in PBS for 15 min. To block the nonspecific binding of antibodies the slides were incubated 1 hour at RT with blocking buffer. FSHR was detected by incubating sections sequentially with FSHR323 antibody (3 $\mu\text{g}/\text{ml}$) in blocking buffer for 2 hours at RT and with goat anti-mouse IgG-Alexa 555 (Molecular Probes; dilution 1:750 in blocking buffer for 1 hour). Double labelling experiments have been done with prostate sections incubated with a mixture of FSHR323 antibody (3 $\mu\text{g}/\text{ml}$ in GS-PBS) and the rabbit polyclonal anti-von Willebrand factor, a specific marker of endothelial cells (Sigma; dilution 1:1000). A mixture of goat-anti mouse IgG-Alexa 555 and goat-anti rabbit Ig-Alexa488 (Molecular Probes; dilution 1:750) has been used as secondary antibodies. In some experiments nuclei were detected by incubating slides for 10 min with TOTO-3 (Molecular Probes; dilution 1:1000 in PBS). The slides were mounted in Dako fluorescent mounting medium containing 15 mM sodium azide and examined with a Zeiss 510 Confocal Laser Scanning Microscope. Negative controls consisted of prostate samples incubated only with fluorescent secondary antibody mixtures. Immunofluorescence confocal microscopy was also done on paraffin sections using a similar method except that the concentration of the FSHR323 antibody was 5 $\mu\text{g}/\text{ml}$.

In situ hybridization

To localize the mRNA encoding for FSHR within ECs of prostate cancer and kidney cancer (paraffin-embedded tissues) we used a 45-mer cDNA antisense oligonucleotide (5'- AAT-CCA-GCC-CAT-CAC-CAT-GAT-ACT-GGC-AGC-ATG-GCG-GAG-CTG-CAC - 3') complementary to the 1441-1486 base pair region of the FSHR sequence.³ The 3'-biotinylated

oligonucleotide probe (Eurogentec; Seraing, Belgium) was detected with alkaline phosphatase conjugated streptavidin (DakoCytomation In Situ Hybridization Detection System; Code K0601). The sites of hybridization were visualized by the colorimetric reaction of the enzyme conjugate with a BCIP (5-bromo-4-chloro-3-indolyl phosphate) and NBT (nitro blue tetrazolium) mixture. The tissues were counterstained by immersing slides in 0.5% methyl green in 0.1 M sodium acetate buffer, pH4.2.

Immunoprecipitations followed by SDS-PAGE and western blotting

These experiments were carried out as previously described² by using 200 mg wet prostate tissue as starting material. Briefly, the tissue was frozen in liquid nitrogen and pulverized using mortar and pestle, solubilized by resuspension in 1.5 ml of extraction buffer (20 mM Tris pH 7.4 containing protease inhibitor cocktail (Roche), 0.4 M NaCl, and 1.2% Triton X-100) at 4°C for 2 hours. The insoluble material was removed after centrifugation at 14 000 x g, and the supernatant was supplemented with 3 µg/ml FSHR323 antibody and incubated overnight at 4°C. The receptor antibody complex was captured by addition of 20 µl of Protein A –Sepharose beads (Amersham). After 1 hour of incubation the beads have been pelleted at 1500 x g and washed by 4 centrifugations and resuspensions in 1 ml of extraction buffer. The beads have been resuspended in 30 µl SDS-PAGE buffer and subjected to electrophoresis and transfer to nitrocellulose. The blots have been blocked with 5% defatted dry milk in 20 mM Tris-HCl pH 7.4 and incubated with FSHR18 (5 µg/ml) for 1 hour at RT. After washing and incubation for 1 hour at RT with goat anti-mouse IgG-peroxidase (Sigma, 1:10,000), the blots have been washed and developed using the ECL reagents from Amersham.

Binding in situ of anti-FSHR-gold to mouse tumor ECs

Male nude mice have been injected in the flank with 200 μ l of 50% Matrigel containing 2×10^6 LNCaP cells. After 3 months, when the tumors reached approx. 1 cm diameter, the mice have been anesthetized and the blood was removed by systemic perfusion with PBS using the left ventricle as inlet and the right atrium as outlet. Anti-FSHR antibodies have been coupled to 5 nm colloidal gold.⁴ The conjugate ($A_{550\text{nm}}=0.1$) in PBS containing 50 μ g/ml nonimmune mouse IgG2a was perfused in mice initially at 3 ml/minute (5 ml) and subsequently in portions of 0.5 ml every minute for 20 minutes. The unbound gold conjugate was washed by perfusion with 20 ml PBS at 3 ml/ minute, and the vasculature was fixed by perfusion for 10 min with a mixture of 4% paraformaldehyde and 2.5% glutaraldehyde in 0.1 M HCl-cacodylate buffer, pH 7.3. The tissues have been processed for electron microscopy.⁴

Results

FSHR expression in non-malignant inflammatory, regenerative and proliferative tissues

We investigated also if FSHR is expressed by ECs in some chronic inflammatory disorders of distinct etiopathogenic origin (rheumatoid arthritis (3 cases), psoriasis (5 cases), Crohn's disease (6 cases) and chronic pancreatitis (6 cases), in which angiogenesis is known to occur.^{5,6} (In psoriasis angiogenesis is thought to be essential for the pathogenesis of the disease^{7,8}). In none of these disorders endothelial FSHR was detected (Figure 3Be,f in the main text and **Figure 5a,b**). In another situation where angiogenesis and inflammation occur, granulation tissue from wounds of breast (4 cases), colon (4 cases), and calf muscles (1 case), FSHR was also absent (**Figure 5c**).

In contrast to the above cases, in placentas (4 cases) almost all vessels are intensely stained (**Figure 5d**). Interestingly, placentas and tumors have common features⁹ that may be relevant for the vascular FSHR expression. Similar to the invasion by the tumor of the

adjacent normal tissues, the developing placenta invades the uterus. Both cancer cells and cells of the developing placenta create a microenvironment supportive of both immunological privilege and angiogenesis. The fetus is a semiallogeneic tissue, and the placenta creates a fetomaternal interface that allows the fetus to escape the rejection by the maternal immune system. Possibly in a similar fashion, the interface between the tumor and the normal tissue, where we see the FSHR expression, may protect the tumor from immune rejection. It may be also relevant that angiogenesis in the tumors and in the placenta are more dependent on Placental Growth Factor (PlGF) than on VEGF, which puts these two types of angiogenesis mechanisms in a distinct class from other types.¹⁰

References

1. Kononen J, Bubendorf L, Kallioniemi A, et al. Tissue microarrays for highthroughput molecular profiling of tumor specimens. *Nat Med* 1998;4:844-7.
2. Vannier B, Loosfelt H, Meduri G, Pichon C, Milgrom E. Anti-human FSH receptor monoclonal antibodies: immunochemical and immunocytochemical characterization of the receptor. *Biochemistry* 1996;35:1358-66.
3. Böckers TM, Nieschlag E, Kreutz MR, Bergmann M. Localization of follicle-stimulating hormone (FSH) immunoreactivity and hormone receptor mRNA in testicular tissue of infertile men. *Cell Tissue Res* 1994;278:595-600.
4. Vu Hai MT, Lescop P, Loosfelt H, Ghinea N. Receptor-mediated transcytosis of follicle stimulating hormone through the rat testicular microvasculature. *Biol Cell* 2004;96:133-44.
5. Costa C, Incio J, Soares R. Angiogenesis and chronic inflammation: cause or consequence? *Angiogenesis* 2007;10:149-66.

6. Kuehn R, Lelkes PI, Bloechle C, Niendorf A, Izbicki JR. Angiogenesis, angiogenic growth factors, and cell adhesion molecules are upregulated in chronic pancreatic diseases: angiogenesis in chronic pancreatitis and in pancreatic cancer. *Pancreas* 1999;18:96-103.
7. Campanati A, Goteri G, Simonetti O, et al. Angiogenesis in psoriatic skin and its modifications after administration of etanercept: videocapillaroscopic, histological and immunohistochemical evaluation. *Int J Immunopathol Pharmacol* 2009;22:371-7.
8. Heidenreich R, Röcken M, Ghoreschi K. Angiogenesis drives psoriasis pathogenesis. *Int J Exp Pathol* 2009;90:232-48.
9. Holtan SG, Creedon DJ, Haluska P, Markovic SN. Cancer and pregnancy: parallels in growth, invasion, and immune modulation and implications for cancer therapeutic agents. *Mayo Clin Proc* 2009;84:985-1000.
10. Fischer C, Jonckx B, Mazzone M, et al. Anti-PlGF inhibits growth of VEGF(R)-inhibitor-resistant tumors without affecting healthy vessels. *Cell* 2007;131:463-75.

Figure legends

Figure 1. Negative control experiments. Blood vessels (arrows) in prostate cancer tissues do not show any signal after incubation with either mouse IgG of the same class as FSHR323 (IgG2a, Sigma M9144) as primary antibody (a) or only with the secondary antibody (b). Bar: 25 μ m.

Figure 2. Two other anti-FSHR monoclonal antibodies confirm the expression of FSHR by tumor ECs. Immunohistochemistry was performed on paraffin sections of human prostate tissues using the anti-FSHR monoclonal antibody 190 (a,b) or FSHR225 (c,d) followed by a secondary peroxidase-coupled antibody. Representative images from a Gleason score 6 prostate tumor shows staining of vascular ECs (arrows in panel a and c), while blood vessels of normal prostate tissue are FSHR-negative (arrows in b and d). Bars: 20 μ m.

Figure 3. Normal control tissue sections incubated with FSHR323 do not reveal any FSHR expression. Blood vessels (arrows) in normally appearing tissues located further than 10 mm outside the tumors, in the specimens obtained by surgery performed for tumor removal for breast (a), lung (b), liver (c), colon (d), pancreas (e), stomach (f), urinary bladder (g) and kidney (h). Bars: 25 μ m.

Figure 4. Positive controls for FSHR323 staining: Sertoli cells (SC) in the normal testis tissue (a), and granulosa cells (GC) in the normal ovary (b), known to express FSHR, show the expected staining. A faint FSHR signal is visible in the blood vessels present in the same images (arrows). Bars: 25 μ m.

Figure 5. FSHR expression in inflammatory, reparative and proliferative tissues. FSHR is not expressed by the ECs in psoriasis (a), Crohn's disease (b), and granulation tissue (c). Arrows – FSHR-negative vessels. In placenta (d) all vessels express strongly FSHR (arrows). Bar: 100 μ m

Figure 6. ECs in xenograft tumors in mice express FSHR. Paraffin sections from tumors generated by injection of human prostate tumors cells (LNCaP cells) in nude mice have been probed with biotinylated anti-FSHR followed by streptavidin-peroxidase. Vascular ECs are stained (arrows). Bar: 20 μ m.

Figure 7. FSHR323-gold particles introduced by perfusion in the mouse vasculature are rarely visible in the subendothelial space in the tumor. Particles appear infrequently in the subendothelial space adjacent to the endothelial channels (a) and as massive accumulations in the interstitial space (b). EC, endothelial cell; is, interstitial space; ss, subendothelial space. Bars: 50 nm.

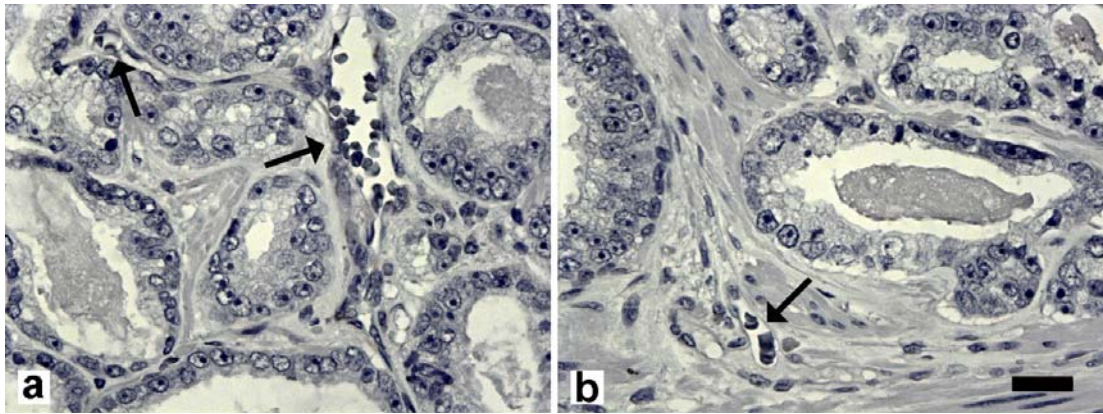


Figure 1

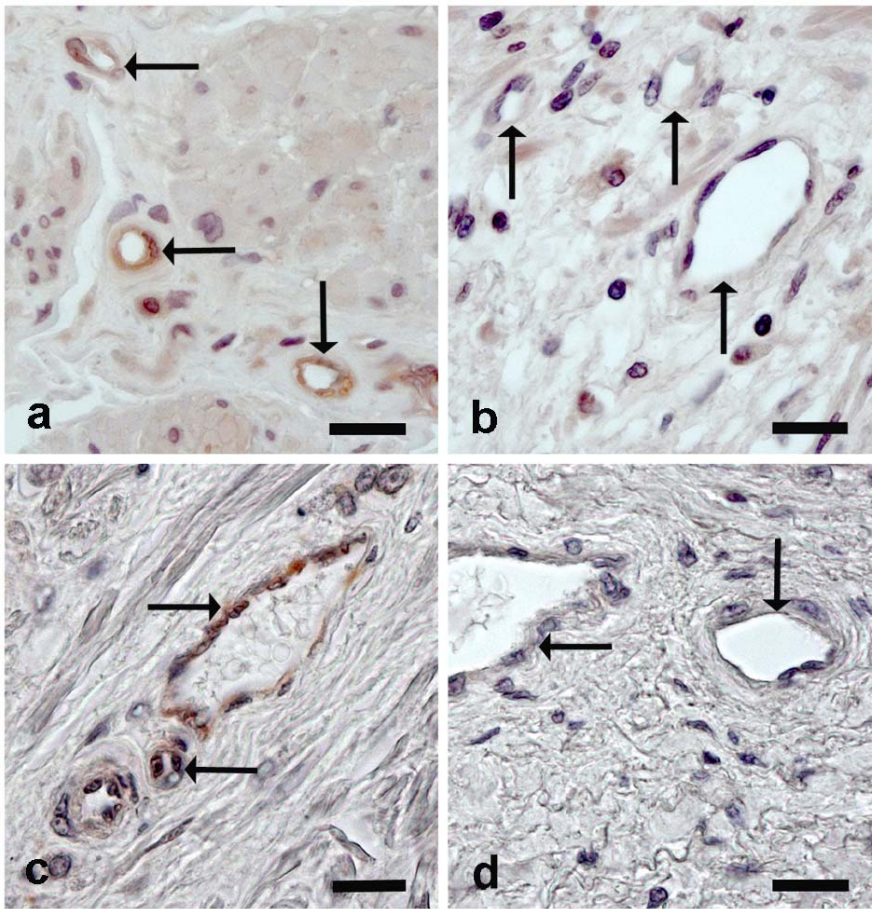


Figure 2

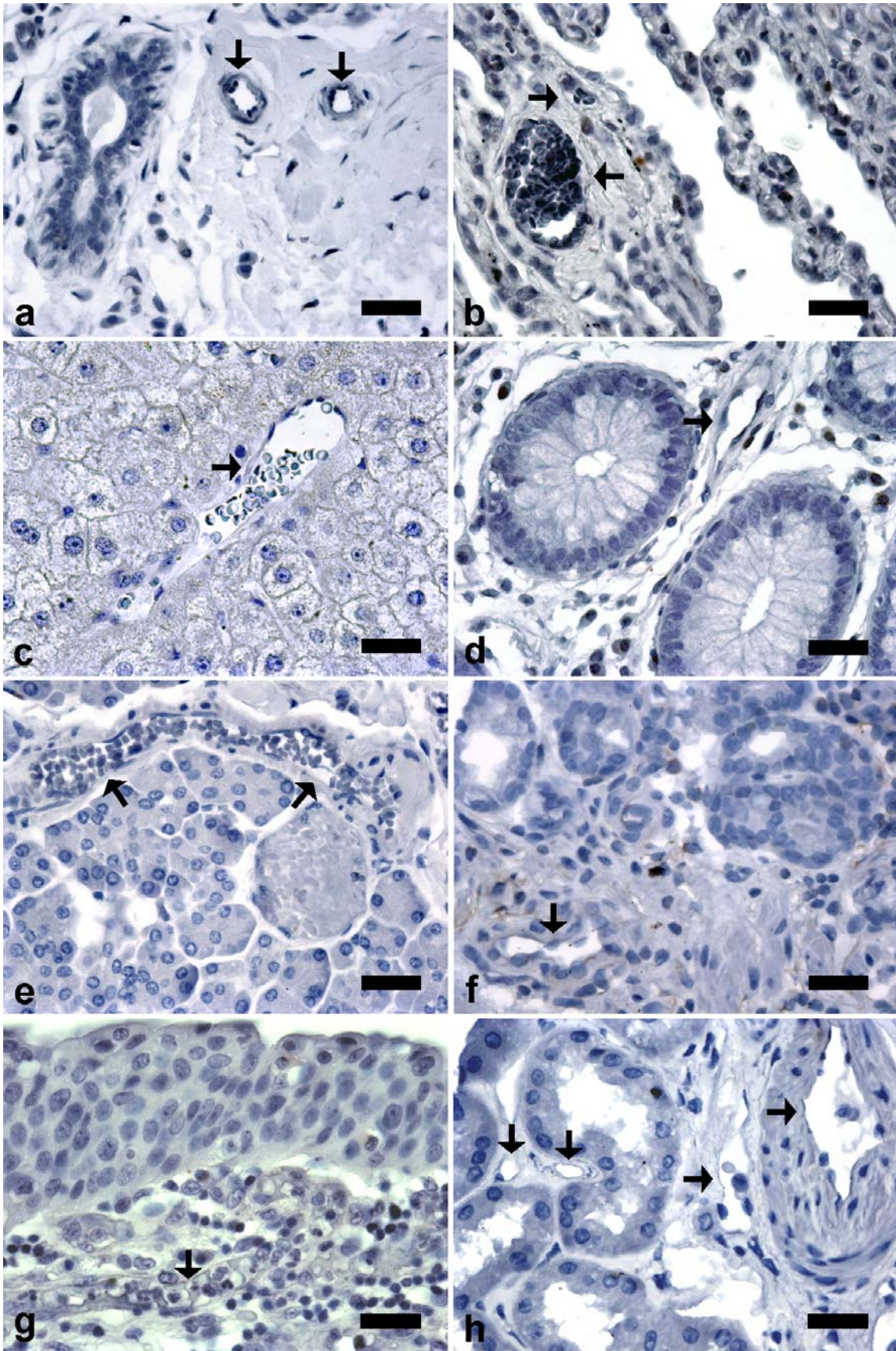


Figure 3

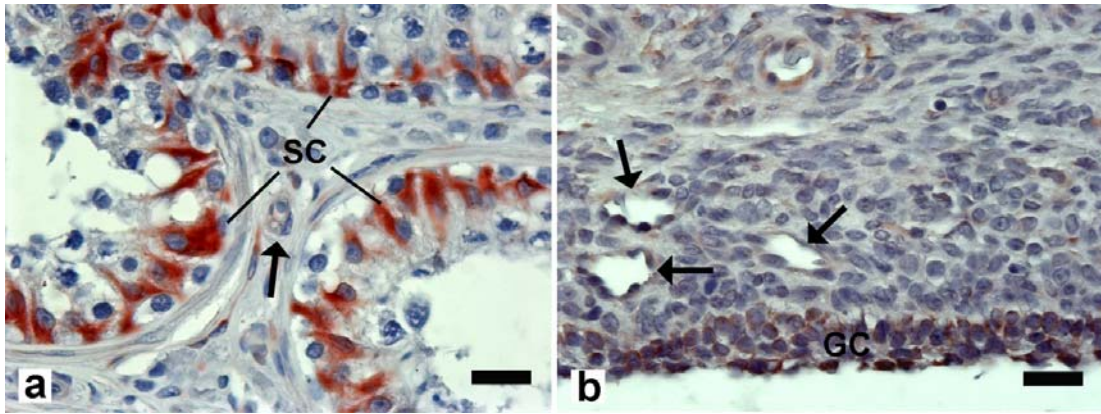


Figure 4

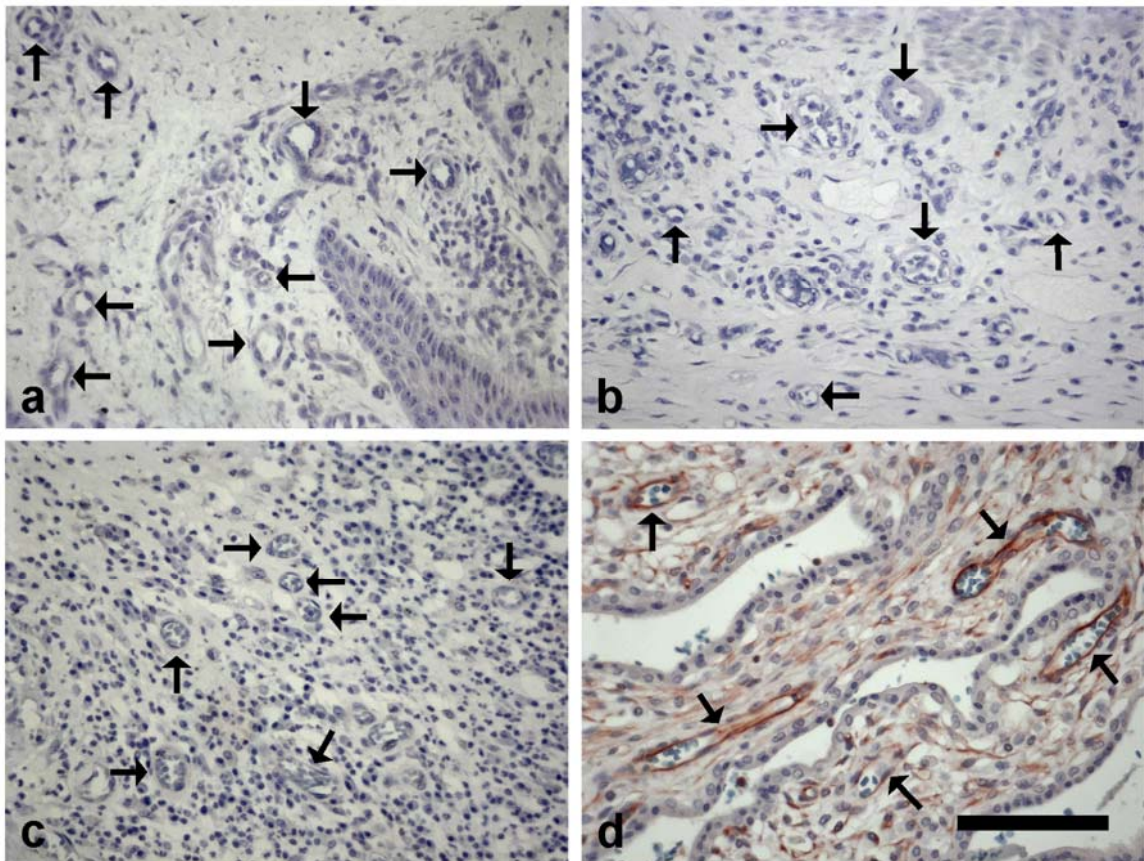


Figure 5

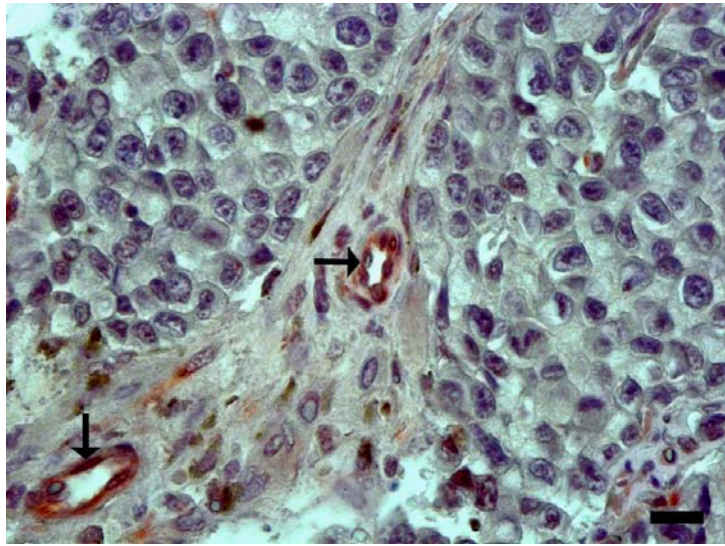


Figure 6

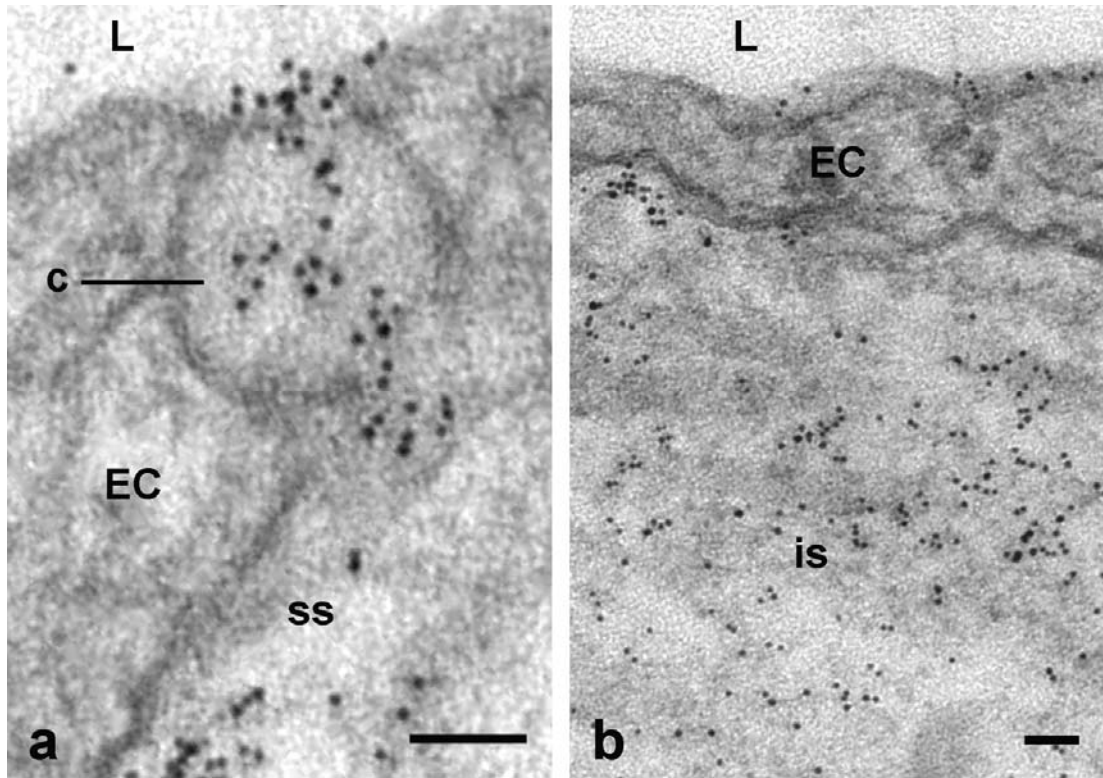


Figure 7

Table 1

TUMOR		No. of Patients	
HISTOPATHOLOGICAL TYPE		F	M
PROSTATE	Adenocarcinomas		773
	Benign hyperplasia		330
BREAST	In situ carcinomas	56	
	Invasive carcinomas	112	
COLON	Adenocarcinomas	6	9
PANCREAS	Adenocarcinomas	27	36
URINARY BLADER	In situ urothelial carcinomas	62	64
	Urothelial translational cell carcinomas	41	36
KIDNEY	Clear cell renal cell carcinomas	25	39
LUNG	Adenocarcinomas	9	6
LIVER	Hepatocellular carcinomas	4	11
STOMACH	Adenocarcinomas	3	3
TESTIS	Seminomas		5
	Sertoli cell carcinomas		1
	Leydig cell tumors		2
OVARY	Epithelial carcinomas	6	